



1
2
3
4
5
6
7
8
9
10
11
12
13
14
15
16
17
18
19
20
21
22
23
24
25
26
27
28
29
30
31
32
33
34
35
36
37
38

Contributions of residential coal combustion to the air quality in Beijing-Tianjin-Hebei (BTH), China: A case study

Xia Li^{1,3}, Jiarui Wu¹, Miriam Elser², Junji Cao¹, Tian Feng¹, Imad El-Haddad², Rujin Huang¹, Xuexi Tie², André S. H. Prévôt³, and Guohui Li^{2*}

¹Key Lab of Aerosol Chemistry and Physics, SKLLQG, Institute of Earth Environment, Chinese Academy of Sciences, Xi'an, China

²Laboratory of Atmospheric Chemistry, Paul Scherrer Institute, 5232 Villigen, Switzerland

³University of Chinese Academy of Science, Beijing, China

*Correspondence to: Guohui Li (ligh@ieecas.cn)

Abstract: In the present study, the WRF-CHEM model is used to evaluate contributions of the residential coal combustion (RCC) emission to the air quality in Beijing-Tianjin-Hebei (BTH) during persistent air pollution episodes from 9 to 25 January 2014. In general, the predicted temporal variations and spatial distributions of the air pollutants mass concentrations are in good agreement with observations at monitoring sites in BTH. The WRF-CHEM model also reasonably well reproduces the temporal variations of aerosol species compared with the AMS measurements in Beijing. The RCC emission plays an important role in the haze formation in BTH, contributing about 23.1% of PM_{2.5} (fine particulate matter) and 42.6% of SO₂ during the simulation period on average. Organic aerosols dominate PM_{2.5} from the RCC emission, with a contribution of 42.8%, followed by sulfate (17.1%). The air quality in Beijing is remarkably improved when the RCC emission in BTH and its surrounding areas is excluded in simulations, with a 30% decrease of PM_{2.5} concentrations. However, when only the RCC emission in Beijing is excluded, the Beijing's PM_{2.5} level is decreased by 18.0% on average. Our results suggest that implementation of the residential coal replacement by clean energy sources in Beijing is beneficial to the Beijing's air quality, but is not expected to bring back the blue sky to Beijing. Should the residential coal replacement be carried out in BTH and its surrounding areas, the air quality in Beijing would be improved remarkably. Further studies need be conducted considering the uncertainties in the emission inventory and meteorological fields.



39 1 Introduction

40 Over the several past decades, China has experienced rapid economic growth,
41 accompanied by accelerating industrialization and urbanization, which have seriously
42 deteriorated air quality (e.g., R. Zhang et al., 2009; X. Zhang et al., 2012; L. Zhang et al., 2015).
43 Recently, the haze pollution has become the primary concern about the air quality in most key
44 regions and cities in China, especially in Beijing-Tianjin-Hebei (BTH) and Yangtze River Delta
45 (YRD) (e.g., Wang et al., 2005; An et al., 2007; Wang et al., 2014; Chen et al., 2016; Gao et
46 al., 2016). The severe and persistent haze pollution with high concentrations of fine particulate
47 matter ($PM_{2.5}$) and the consequent low visibility, is mainly caused by heavy anthropogenic
48 emissions and unfavorable synoptic situations (e.g., Seinfeld and Pandis, 2006; Lei et al., 2011;
49 Lv et al., 2016; Wang et al., 2016; Zíková et al., 2016). According to the China's Ministry of
50 Environment Protection (MEP), the annual mean $PM_{2.5}$ concentration was $102 \mu\text{g m}^{-3}$ in 2013
51 and $93 \mu\text{g m}^{-3}$ in 2014 in BTH, far beyond the World Health Organization (WHO) interim
52 target-1 of $35 \mu\text{g m}^{-3}$ for the annual mean $PM_{2.5}$ concentration and also the secondary class
53 standard in the China's new National Ambient Air Quality Standard (NAAQS, GB3095-2012).
54 Therefore, the Chinese State Council has issued the "Atmospheric Pollution Prevention and
55 Control Action Plan (APPCAP)" in September 2013 to reduce $PM_{2.5}$ by up to 25% by 2017
56 relative to 2012 levels. Since implementation of the APPCAP, stringent control strategies have
57 been carried out to reduce the pollutants emissions from power plants, industries and the
58 transportation (Sheehan et al., 2014; Liu et al., 2015; Yang et al., 2016). Control strategies have
59 also been implemented to reduce residential emissions to the air quality, but the mitigation
60 effect is still lack of evaluation constrained by observations.

61 The air pollution in China is a typical coal-smoke pollution, which is considered to be
62 associated closely with China's special energy consumption structure (e.g., Quan et al., 2014;
63 Archernicholls et al., 2016; Liu et al., 2016; Xue et al., 2016). Coal plays a key role in China's



64 energy structure, and as the most abundant and a relatively cheap energy resource, coal is
65 regarded as a dominant energy supply in China in the foreseeable future. According to the BP
66 statistical review of world energy, from 1980s to the present day, the proportion of coal in
67 China' primary energy production and consumption has been around 70%, which is much
68 higher than that of around 20% in OECD (Organization for Economic Co-operation and
69 Development) countries. Entering the 21 centuries, the coal consumption in China has
70 increased sharply, and by 2013, China's coal consumption has accounted for 50.3% of the
71 global coal consumption, which was 4.2 and 6.7 times higher than the United States and the
72 European Union, respectively. In 2013, coal is responsible for 79%, 54%, 40%, 35%, 40%, and
73 17% of the SO₂, NO_x, PM₁₀, PM_{2.5}, BC, and OC emissions in China, respectively (Ma et al.,
74 2016).

75 Residential coal combustion (RCC) is recognized as a significant source of air pollution,
76 affecting both local and regional air quality and posing serious threat to human health and
77 environment by releasing hazardous air pollutants (HAPs), including PM, black carbon (BC),
78 organic carbon (OC), SO₂, NO_x, CO, CO₂, and polycyclic aromatic hydrocarbons (PAHs) (e.g.,
79 Wornat et al., 2001; Ge et al., 2004; Zhi et al., 2008; Shen et al., 2010; Cheng et al., 2016; Li
80 et al., 2016). Chemical transport models have been used to investigate the contribution of the
81 RCC emission to the ambient air pollution in China. Using the CMAQ model, Y. Xue et al.
82 (2016) have shown that the contributions of the RCC emission to the mass concentrations of
83 PM₁₀, SO₂, NO_x, and CO are 11.6%, 27.5%, 2.8%, and 7.3%, respectively, during the winter
84 heating season of 2012 in Beijing. Simulations using the GEOS-CHEM model by Q. Ma et al.
85 (2016) have demonstrated that the coal combustion contributes 40% of the total PM_{2.5}
86 concentration on national average in 2013. Among major coal-burning sectors, industrial coal
87 burning contributes 17% of the PM_{2.5} concentrations, followed by power plants (9.8%) and
88 domestic sector (4.0%). J. Liu et al. (2016) have used the WRF-CHEM model to simulate the



89 air pollution in BTH in January and February 2010, indicating that annual elimination of
90 residential sources in BTH reduces emissions of primary $PM_{2.5}$ by 32%, compared with 5%,
91 6%, and 58% of transportation, power plants, and industrial sectors, respectively.

92 In the present study, we use the Weather Research and Forecasting model coupled with
93 chemistry (WRF-CHEM) to evaluate the contribution of the RCC emission to the air quality in
94 BTH during persistent air pollution episodes from 9 to 25 January 2014. The WRF-CHEM
95 model configurations and methodology are described in Section 2. Model results and
96 discussions are represented in Section 3, and conclusions are given in Section 4.

97

98 **2 Model and Methodology**

99 **2.1 WRF-CHEM model and configurations**

100 The WRF-CHEM model used in the study is developed by Li et al. (2010, 2011a, b, 2012)
101 at the Molina Center of Energy and the Environment, based on the previous studies (Grell et
102 al., 2005; Fast et al., 2006). The wet deposition follows the method used in the CMAQ module
103 and the dry deposition of chemical species is parameterized following Wesely (1989). The
104 photolysis rates are calculated using the FTUV (fast radiation transfer model), including the
105 aerosol and cloud effects on photolysis (Tie et al., 2003; Li et al., 2005, 2011a). The inorganic
106 aerosols are calculated using ISORROPIA Version 1.7 (Nenes, 1998). The secondary organic
107 aerosol (SOA) is predicted using the volatility basis-set (VBS) modeling method, with
108 contributions from glyoxal and methylglyoxal. Detailed information can be found in Li et al.
109 (2010, 2011b).

110 Persistent air pollution episodes from 9 to 25 in January 2014 in BTH are simulated using
111 the WRF-CHEM model. During the study period, the averaged $PM_{2.5}$ concentration in BTH is
112 $161.9 \mu\text{g m}^{-3}$, with a maximum of $323.5 \mu\text{g m}^{-3}$. The average temperature and relative humidity
113 in Beijing during the period is -1.7°C and 32.3%, respectively, and the average wind speed is



114 about 2.8 m s^{-1} . The model simulation domain is shown in Figure 1, and detailed model
115 configurations can be found in Table 1.

116 2.2 Statistical methods for comparisons

117 In the present study, we use the mean bias (MB), root mean square error (RMSE) and
118 index of agreement (IOA) to validate the WRF-CHEM model performance in simulating air
119 pollutants and aerosol species against observations and measurements. IOA describes the
120 relative difference between the model prediction and observation, ranging from 0 to 1, with 1
121 indicating perfect agreement of the prediction with the observation.

$$122 \quad MB = \frac{1}{N} \sum_{i=1}^N (P_i - O_i)$$

$$123 \quad RMSE = \left[\frac{1}{N} \sum_{i=1}^N (P_i - O_i)^2 \right]^{\frac{1}{2}}$$

$$124 \quad IOA = 1 - \frac{\sum_{i=1}^N (P_i - O_i)^2}{\sum_{i=1}^N (|P_i - \bar{P}| + |O_i - \bar{O}|)^2}$$

125 Where P_i and O_i are the predicted and observed pollutant concentrations, respectively. N is
126 the total number of the predictions used for comparisons, and \bar{P} and \bar{O} represent the average
127 of predictions and observations, respectively.

128 2.3 Pollutants measurements

129 The hourly near-surface CO, SO₂, NO₂, O₃, and PM_{2.5} mass concentrations released by the
130 China's Ministry of Environmental Protection can be downloaded from the website
131 <http://www.aqistudy.cn/>. The sulfate, nitrate, ammonium, and organic aerosols (OA) have been
132 measured by the Aerodyne High Resolution Time-of-Flight Aerosol Mass Spectrometer (HR-
133 ToF-AMS) with a novel PM_{2.5} lens from 9 to 26 January 2014 at the Institute of Remote
134 Sensing and Digital Earth (IRSDE), Chinese Academy of Sciences (40.00°N, 116.38°E) in
135 Beijing (Figure 1) (Williams et al., 2013). The Positive Matrix Factorization (PMF) technique
136 is used with constraints implemented in SoFi (Canonaco et al., 2013) to analyze the sources of
137 OA and five components are separated by their mass spectra and time series. The components



138 include hydrocarbon-like OA (HOA), cooking OA (COA), biomass burning OA (BBOA), coal
139 combustion OA (CCOA), and oxygenated OA (OOA). HOA, COA, BBOA, and CCOA are
140 interpreted for surrogates of primary OA (POA), and OOA is a surrogate for SOA. Detailed
141 information about the HR-ToF-AMS measurements and data analysis can be found in Elser et
142 al. (2016).

143

144 **3 Results and discussions**

145 **3.1 Model performance**

146 For the discussion convenience, we have defined the reference simulation in which the
147 emissions from various sources are considered (hereafter referred to as REF), and results from
148 the reference simulation are compared to observations in BTH.

149 **3.1.1 Air pollutants simulations in BTH**

150 Figure 2 presents the distributions of predicted and observed near-surface mass
151 concentrations of PM_{2.5}, O₃, NO₂, and SO₂ along with the simulated wind fields averaged from
152 9 to 25 January 2014 in BTH. Generally, the predicted PM_{2.5} spatial pattern is well consistent
153 with the observations at the ambient monitoring sites in BTH. The WRF-CHEM model
154 reasonably well reproduces the high PM_{2.5} concentrations exceeding 150 µg m⁻³ in the plain
155 region of BTH. Apparently, during the simulation period, the weak or calm winds in the plain
156 region of BTH facilitate the accumulation of PM_{2.5}, causing severe air pollution. The average
157 simulated PM_{2.5} concentrations exceed 250 µg m⁻³ in the south of Hebei, which is generally in
158 good agreement with observations. The observed and simulated O₃ concentrations are rather
159 low in the plain region of BTH with the high PM_{2.5} level, varying from 10 to 30 µg m⁻³. There
160 are several reasons for the low O₃ concentrations in the plain region of BTH. Firstly, during
161 wintertime, the insolation is weak in the north of China, unfavorable for the O₃ photochemical
162 production. Additionally, high PM_{2.5} concentrations and frequent occurrence of clouds during



163 haze days further attenuate the incoming solar radiation in the planetary boundary layer (PBL),
164 decreasing the O₃ level. Secondly, calm or weak winds indicate stagnant situations, lacking the
165 O₃ transport from outside of BTH. Thirdly, high nitrogen oxides (NO_x=NO+NO₂) emissions
166 cause titration of O₃, which is shown by the high NO₂ concentrations in the plain region of
167 BTH. The elevated NO₂ and SO₂ concentrations are observed and simulated in the plain region
168 of BTH, particularly in cities and their surrounding areas, ranging from 50 to 100 μg m⁻³ and
169 50 to 150 μg m⁻³, respectively. It is worth noting that the simulated NO₂ is generally distributed
170 evenly in the plain region of BTH, indicating the dominant contribution of area sources.

171 Figure 3 presents the diurnal profiles of observed and simulated near-surface PM_{2.5}, O₃,
172 NO₂, SO₂, and CO mass concentrations averaged over all monitoring sites in BTH from 9 to
173 25 January 2014. The WRF-CHEM model well reproduces the diurnal variations of the PM_{2.5}
174 mass concentrations compared with the observations in BTH during the simulation period. The
175 *MB* and *RMSE* is -2.7 and 40.9 μg m⁻³, respectively, and the *IOA* is 0.94. During the three haze
176 episodes occurred in BTH, the model generally replicate well the haze developing stage, but
177 tends to underestimate the PM_{2.5} concentration compared to observations during the haze
178 dissipation stage. One of the most possible reasons is the uncertainty of the simulated
179 meteorological fields, which determine the formation, transformation, diffusion, transport, and
180 removal of the air pollutants in the atmosphere (Bei et al., 2012, 2013). Should the predicted
181 winds be intensified earlier than observations in BTH during the haze dissipation stage, the
182 simulated PM_{2.5} concentrations would fall off earlier, causing the model underestimation. The
183 predicted NO₂ diurnal variations are generally well consistent with the observations, with a *MB*
184 of 4.2 μg m⁻³ and an *IOA* of 0.93. The model also reasonable well yields the SO₂ and CO
185 temporal variations with the *IOA* exceeding 0.85. However, the *RMSE* for SO₂ is rather large,
186 showing considerable dispersions of the SO₂ simulations. A great deal of SO₂ are emitted from
187 power plants or agglomerated industrial zones, which can be regarded as point sources, so the



188 transport of SO₂ is more sensitive to uncertainties of the simulated wind fields.

189 3.1.2 Aerosol species simulations in Beijing

190 Figure 4 presents the temporal profiles of measured and simulated OA, CCOA, sulfate,
191 nitrate, and ammonium concentrations at IRSDE site in Beijing from 9 to 25 January 2014.

192 The model generally performs reasonably well in simulating the diurnal variations of the
193 aerosol species compared to the HR-ToF-AMS measurements, with *IOAs* exceeding 0.80. As
194 a primary species, OA is primarily determined by direct emissions from various sources,
195 including vehicles, cooking, biomass burning, coal combustion, and transport from outside of
196 Beijing, so uncertainties in emissions and the simulated meteorological fields markedly
197 influence the OA simulations (Bei et al., 2017). Although the *IOA* for OA is 0.84, the model
198 slightly overestimates the OA concentrations with a *MB* of 5.1 µg m⁻³, and the dispersion of
199 OA simulations is also large, with a *RMSE* of 42.3 µg m⁻³. In addition, the model fails to
200 reproduce the measured OA peaks during the nighttime on 11 and 17 January 2014, which is
201 perhaps caused by the emission uncertainty. The model also generally tracks the measured
202 diurnal variations of CCOA concentrations, with an *IOA* of 0.81. The model frequently
203 underestimates or overestimates the CCOA concentrations and is also subject to missing the
204 observed CCOA peaks. The CCOA is mainly emitted from industries and the residential coal
205 combustion. In general, the CCOA emissions from industries have clear diurnal variations, and
206 vice versa for those from residential coal combustion, causing large model biases for the CCOA
207 simulation. The simulated diurnal variations of sulfate, nitrate, and ammonium are also in good
208 agreement with the observations, with *IOAs* of 0.83, 0.87, and 0.90, respectively. The model
209 considerably overestimates the inorganic aerosol concentrations from 16 to 18 January. One of
210 the possible reasons is the decreased emissions, particularly from industries before the Chinese
211 New Year, which are not reflected in the emission inventory used in the study.

212 Figure 5 presents the contributions of aerosol species to the simulated PM_{2.5} concentration



213 in BTH and Beijing averaged from 9 to 25 January 2014. The simulated $PM_{2.5}$ mass
214 concentration averaged during the simulation period is 111.6 and $97.7 \mu\text{g m}^{-3}$ in BTH and
215 Beijing, respectively. OA is the dominant constituent of the simulated $PM_{2.5}$, consisting of
216 around 43% of the $PM_{2.5}$ mass in BTH. Although the simulated O_3 concentration is low, the
217 secondary aerosols, including SOA, sulfate, nitrate, and ammonium still make up about 50%
218 of the $PM_{2.5}$ mass, in which the contribution of sulfate, nitrate, and ammonium is 11.3%, 12.4%,
219 9.6%, and 7.5%, respectively. Elemental carbon and the unspecified aerosol species account
220 for 7.5% and 16.2% of the $PM_{2.5}$ mass, respectively. In Beijing, OA, sulfate, nitrate, and
221 ammonium constitutes 44.1%, 10.6%, 14.0%, and 9.1% of the $PM_{2.5}$ mass, respectively, during
222 the simulation period, which is close to the source apportionment results obtained by Huang et
223 al. (2014) during the wintertime of 2013. It is worth noting that the simulated sulfate
224 contribution to the $PM_{2.5}$ mass in Beijing is lower than the source apportionment result in
225 Huang et al. (2014), and vice versa for the nitrate aerosol. Implementation of the APPCAP
226 since 2013 September has considerably decreased SO_2 emissions in BTH, lowering the sulfate
227 formation. Additionally, the decrease of the sulfate aerosol reduces its competition for
228 ammonia in the atmosphere, facilitating the nitrate formation.

229 The good agreements of the simulated mass concentrations of air pollutants with
230 observations at ambient monitoring sites in BTH and aerosol species with HR-ToF-AMS
231 measurements in Beijing show that the simulated wind fields and emission inventory used in
232 present study are generally reasonable, providing a reliable base for the further evaluation.

233 **3.2 Contributions of the RCC emission to the air quality in BTH**

234 The contribution of the residential coal combustion (RCC) emission to the air quality in
235 BTH is investigated by the sensitivity study without RCC emissions in BTH and its
236 surrounding areas compared to the reference simulation (hereafter we define the sensitivity
237 simulation as SEN-BTH). Figure 6 shows the spatial distribution of the average contribution



238 of the RCC emission in BTH and its surrounding areas to the $PM_{2.5}$ concentrations during the
239 simulation period (defined as (REF – SEN-BTH)). The RCC emission plays an important role
240 in the $PM_{2.5}$ level in the plain area of BTH, with a contribution varying from 30 to $70 \mu\text{g m}^{-3}$.
241 Over the mountain areas of BTH, the contribution of the RCC emission to the $PM_{2.5}$
242 concentration is generally less than $10 \mu\text{g m}^{-3}$.

243 Table 2 presents the average change of air pollutants mass concentrations during the
244 simulation period in BTH and Beijing. The average $PM_{2.5}$ concentration is $111.6 \mu\text{g m}^{-3}$ in BTH
245 in the REF case and decreased to be $85.8 \mu\text{g m}^{-3}$ in the SEN-BTH case when the RCC emission
246 is excluded. The RCC emission contributes about 23.1% of $PM_{2.5}$ mass in BTH on average. In
247 addition, the RCC emission is an important SO_2 and CO source, contributing about 35.8% of
248 SO_2 and 22.5% of CO. The RCC emission does not substantially influence the NO_2 level in
249 BTH, with a contribution of 4.2%. When the RCC emission is not considered in the SEN-BTH
250 case, the O_3 concentration is slightly increased due to decrease of the NO_2 concentration. The
251 $PM_{2.5}$ concentration is decreased by around 30% in Beijing on average when the RCC emission
252 in BTH is excluded, showing that the air quality in Beijing would be remarkably improved if
253 the residential coal in BTH and its surrounding areas could be replaced by other clean energy
254 sources, such as natural gas or electricity. Furthermore, the RCC emission in BTH and its
255 surrounding areas contributes about 42.6% of SO_2 and 26.5% of CO in Beijing.

256 Figure 7 shows the average chemical composition of $PM_{2.5}$ contributed by the RCC
257 emission in BTH and Beijing during the simulation period. The RCC emission contributes
258 about $25.8 \mu\text{g m}^{-3}$ $PM_{2.5}$ in BTH on average, of which about 42.8% is from OA. The sulfate
259 aerosol constitutes 17.1% of $PM_{2.5}$ contributed by the RCC emission, exceeding the
260 contribution from unidentified aerosol species (15.8%), black carbon (11.5%), ammonium
261 (9.5%) and nitrate (3.3%) aerosol. The results indicate that the priority to mitigate effects of
262 the RCC emission on the air quality in BTH is to decrease the emissions of OA and SO_2 from



263 RCC. In Beijing, OA is still the major contributor to $PM_{2.5}$ from the RCC emission, accounting
264 for about 48.5% which is more than that averaged in BTH. The sulfate and ammonium
265 contribution to $PM_{2.5}$ from the RCC emission is 13.3% and 7.2%, respectively, less than those
266 averaged in BTH. The chemical composition of $PM_{2.5}$ from the RCC emission in Beijing shows
267 more contribution of OA and less contribution of SO_2 from Beijing local RCC emission.

268 **3.4 Contributions of RCC emissions to the air quality in Beijing**

269 As the capital of China, the air quality in Beijing often becomes the focus of attention in
270 China or globally. Beijing is situated at the northern tip of the North China Plain (NCP), one
271 of the most polluted areas in China, caused by rapid industrialization and urbanization (Zhang
272 et al., 2013). In addition, Beijing is surrounded from the southwest to the northeast by the
273 Taihang Mountains and the Yanshan Mountains which block the dispersion of air pollutants
274 when the south or east winds are prevalent in NCP (Long et al., 2016). Therefore, except the
275 contribution of local emissions, the air quality in Beijing is also substantially influenced by the
276 transport of air pollutants from outside (Wu et al., 2017).

277 Since implementation of the APPCAP issued in September 2013, Beijing has carried out
278 aggressive emission control strategies to improve the air quality. Great efforts have been made
279 to replace the coal used in residential living by natural gas or electricity, which is highly
280 anticipated to clean the air in Beijing. However, frequent occurrence of heavy haze with
281 extremely high levels of $PM_{2.5}$ during the wintertime of 2015 and 2016 has caused controversial
282 issue about the effect of the coal replacement plan in Beijing. Therefore, a further sensitivity
283 study has been performed, in which only the RCC emission in Beijing is excluded (hereafter
284 we define the sensitivity simulation as SEN-PEK) to explore the contribution of the local RCC
285 emission in Beijing to the haze formation. Comparisons of the REF case with the SEN-PEK
286 case show that when the RCC emission is not considered or the residential coal is replaced by
287 other clean energy sources in Beijing, the Beijing's $PM_{2.5}$ level decreases from 97.7 to 80.1 μg



288 m^{-3} or by 18.0% on average during the simulation period. The average decrease of SO_2 and CO
289 concentrations is 24.2% and 19.9%, respectively. Therefore, the coal replacement plan in
290 Beijing can improve the air quality in Beijing considerably, but is not as expected to bring back
291 the blue sky to Beijing.

292 It is still disputatious on whether local emissions or transport from outside dominates the
293 air quality in Beijing (Guo et al., 2010, 2014; Li et al., 2015; Zhang et al., 2015; Wu et al.,
294 2017). Sensitivity studies show that when only the RCC emission in Beijing is excluded in
295 simulations, the $\text{PM}_{2.5}$ level is decreased by 18%, much less than about 30% decrease caused
296 by the exclusion of the RCC emission in BTH and its surrounding areas, showing the important
297 contribution of trans-boundary transport to the air quality in Beijing. Analyses are further made
298 to examine the contribution of the RCC emission in Beijing to the $\text{PM}_{2.5}$ concentrations under
299 different pollution levels. The simulated hourly near-surface $\text{PM}_{2.5}$ concentrations in REF case
300 during the whole episode in Beijing are first subdivided into 6 bins according to the air quality
301 standard in China for $\text{PM}_{2.5}$ (Feng et al., 2016), i.e., 0~35 (excellent), 35~75 (good), 75~115
302 (lightly polluted), 115~150 (moderately polluted), 150~250 (heavily polluted), and greater than
303 250 (severely polluted) $\mu\text{g m}^{-3}$. $\text{PM}_{2.5}$ concentrations in REF case and SEN-PEK case as the
304 bin $\text{PM}_{2.5}$ concentrations in REF case following the grid cells are assembled respectively, and
305 an average of $\text{PM}_{2.5}$ concentrations in each bin is calculated. Figures 8 presents the contribution
306 of the RCC emission in Beijing to the local $\text{PM}_{2.5}$ concentrations. Apparently, the mitigation
307 effect is the best under the good and lightly polluted conditions, and the $\text{PM}_{2.5}$ concentration
308 decreases by around 25% when the RCC emission in Beijing is not considered, indicating that
309 the good and light $\text{PM}_{2.5}$ pollution is mainly caused by local emissions. However, with
310 deterioration of the haze pollution from moderately to severely polluted conditions, the $\text{PM}_{2.5}$
311 contribution of the local RCC emission decreases from 20% to 15%, showing the regional
312 transport of $\text{PM}_{2.5}$.



313

314 **4 Summary and Conclusions**

315 In the present study, persistent air pollution episodes in BTH from 9 to 25 January 2014
316 are simulated using the WRF-CHEM model to evaluate the contributions of the RCC emission
317 to the air quality in BTH. In general, the WRF-CHEM model performs well in simulating the
318 temporal variations and spatial distributions of air pollutants compared to observations over
319 monitoring sites in BTH. The simulated diurnal variations of aerosol species are also in good
320 agreement with the HR-ToF-AMS measurements in Beijing.

321 Sensitivity studies show that, on average, the RCC emission contributes about 23.1% of
322 $PM_{2.5}$ mass concentrations in BTH during the simulation period and is also an important SO_2
323 and CO source, accounting for about 35.8% of SO_2 and 22.5% of CO. OA is the major
324 contributor to $PM_{2.5}$ from the RCC emission, with a contribution of 42.8%, followed by sulfate
325 (17.1%), unidentified aerosol species (15.8%), black carbon (11.5%), ammonium (9.5%) and
326 nitrate (3.3%) aerosol. Exclusion of the RCC emission in BTH and its surrounding areas
327 decreases the $PM_{2.5}$ concentration by around 30% in Beijing, indicating that the air quality in
328 Beijing will be remarkably improved if the residential coal in BTH and its surrounding areas
329 can be replaced by other clean energy sources.

330 When only the RCC emission in Beijing is excluded in simulations, the Beijing's $PM_{2.5}$
331 level decreases by 18.0% on average during the simulation period. Hence, the coal replacement
332 plan in Beijing is beneficial to the Beijing's air quality, but is not as anticipated to bring back
333 the blue sky to Beijing. The mitigation effect of the coal replacement plan on $PM_{2.5}$ in Beijing
334 is the best under the good and lightly polluted conditions, decreasing the $PM_{2.5}$ concentration
335 by around 25%. However, under the heavy or severe haze pollution, the local RCC emission
336 contributes about 15% of $PM_{2.5}$ in Beijing, showing contributions of the regional transport of
337 $PM_{2.5}$.



338 This study mainly aims to quantitatively evaluate the contributions of the RCC emission to
339 the air quality in BTH. Our results suggest that if the residential coal replacement is only
340 implemented in Beijing, the Beijing's air quality will not be improved substantially,
341 considering the impact of trans-boundary transport. Implementation of the residential coal
342 replacement in BTH and its surrounding areas can remarkably improve the Beijing's air quality.
343 Although the WRF-CHEM model reasonably well captures the temporal and spatial variations
344 of air pollutants in BTH and diurnal variations of aerosol species in Beijing, the model biases
345 still exist. Future studies need to be conducted to improve the WRF-CHEM model simulations,
346 considering the rapid changes in anthropogenic emissions since the implementation of the
347 APPCAP. Further sensitivity simulations of various emission mitigation measures also need to
348 be performed to provide efficient emission control strategies to improve the air quality in BTH.

349

350 **5 Data availability**

351 The real-time O₃ and PM_{2.5} concentrations are accessible to the public on the website
352 <http://106.37.208.233:20035/> (China MEP, 2013a). One can also access the historic profiles of
353 the observed ambient air pollutants by visiting <http://www.aqistudy.cn/> (China MEP, 2013b).

354

355 *Acknowledgements.* This work is financially supported by the National Key R&D Plan
356 (Quantitative Relationship and Regulation Principle between Regional Oxidation Capacity of
357 Atmospheric and Air Quality (2017YFC0210000)). Guohui Li is supported by “Hundred
358 Talents Program” of the Chinese Academy of Sciences and the National Natural Science
359 Foundation of China (No. 41661144020).

360

361

362

363

364 **References**

- 365 An, X., Zhu, T., Wang, Z., Li, C., and Wang, Y., 2007. A modeling analysis of a heavy air
366 pollution episode occurred in Beijing. *Atmospheric Chemistry and Physics*, 7(12), 3103-
367 3114, doi: 10.5194/acp-7-3103-2007.
- 368 Archernicholls, S., Carter, E. M., Kumar, R., Xiao, Q., Yang, L., Frostad, J., Forouzanfar, M.
369 H., Cohen, A., Brauer, M., Baumgartner, J., and Wiedinmyer, C., 2016. The regional
370 impacts of cooking and heating emissions on ambient air quality and disease burden in
371 China. *Environmental Science and Technology*, 50(17), 9416-8423, doi:
372 10.1021/acs.est.6b02533.
- 373 Bei, N. F., Li, G. H., Zavala, M., Barrera, H., Torres, R., Grutter, M., Gutierrez, W., Garcia,
374 M., Ruiz-Suarez, L. G., Ortinez, A., Guitierrez, Y., Alvarado, C., Flores, I., and Molina,
375 L. T., 2013. Meteorological overview and plume transport patterns during Cal-Mex 2010.
376 *Atmospheric Environment*, 70, 477-489, doi: 10.1016/j.atmosenv.2012.01.065.
- 377 Bei, N., Li, G., and Molina, L. T., 2012. Uncertainties in SOA simulations due to
378 meteorological uncertainties in Mexico City during MILAGRO-2006 field campaign.
379 *Atmospheric Chemistry and Physics*, 12, 11295-11308, doi: 10.5194/acp-12-11295-2012.
- 380 Bei, N., Wu, J., Elser, M., Feng, T., Cao, J., El-Haddad, I., Li, X., Huang, R., Li, Z., Long, X.,
381 Xing, L., Zhao, S., Tie, X., Prévôt, A. S. H., and Li, G., 2017. Impacts of meteorological
382 uncertainties on the haze formation in Beijing-Tianjin-Hebei (BTH) during wintertime: a
383 case study. *Atmospheric Chemistry and Physics*, 17, 14579-14591, doi: 10.5194/acp-17-
384 14579-2017.
- 385 BP: Statistical Review of World Energy 2016.
- 386 Canonaco, F., Crippa, M., Slowik, J. G., Baltensperger, U., and Prévôt, A. S. H., 2013. Sofi,
387 an IGOR-based interface for the efficient use of the generalized multilinear engine (ME-
388 2) for the source apportionment: ME-2 application to aerosol mass spectrometer data.
389 *Atmospheric Measurement Techniques*, 6(12), 3649-3661, doi: 10.5194/amt-6-3649-
390 2013.
- 391 Corrigan, A. L., Russell, L. M., Takahama, S., Äijälä, M., Ehn, M., Junninen, H., Rinne, J.,
392 Petäjä, T., Kulmala, M., Vogel, A. L., Hoffmann, T., Ebben, C. J., Geiger, F. M., Chhabra,
393 P., Seinfeld, J. H., Worsnop, D. R., Song, W., Auld, J., and Williams, J., 2013. Biogenic
394 and biomass burning organic aerosol in a boreal forest at Hyytiälä, Finland, during
395 HUMPPA-COPEC 2010. *Atmospheric Chemistry and Physics*, 13, 12233-12256, doi:
396 10.5194/acp-13-12233-2013.
- 397 Chen, F. and Dudhia, J., 2001. Coupling an advanced land surface-hydrology model with the
398 Penn State-NCAR MM5 modeling system. Part I: Model implementation and sensitivity.
399 *Monthly Weather Review*, 129(4), 569-585, doi: 10.1175/1520-
400 0493(2001)129<0569:caalsh>2.0.co;2.
- 401 Chen, Y., Schleicher, N., Cen, K., Liu, X., Yu, Y., Zibat, V., Dietze, V., Fricker, M., Kaminski,
402 U., Chen, Y., Chai, F., Norra, S., 2016. Evaluation of impact factors on PM_{2.5} based on
403 long-term chemical components analyses in the megacity Beijing, China. *Chemosphere*,
404 155, 234-42, doi: 10.1016/j.chemosphere.2016.04.052.



- 405 Cheng, M., Zhi, G., Tang, W., Liu, S., Dang, H., Guo, Z., Du, J. H., Du, X. H., Zhang, W. Q.,
406 Zhang, Y. J., and Meng, F., 2016. Air pollutant emission from the underestimated
407 households' coal consumption source in China. *Science of the Total Environment*, 580,
408 641-650, doi: 10.1016/j.scitotenv.2016.12.143.
- 409 Chinese State Council. Atmospheric Pollution Prevention and Control Action Plan, 2013 (in
410 Chinese).
- 411 Chou, M. D. and Suarez, M. J., 1999. A solar radiation parameterization for atmospheric
412 studies, NASA/TM-10460. *Nasa Technical memo*, 15.
- 413 Chou, M. D. and Suarez, M. J., 2001. A thermal infrared radiation parameterization for
414 atmospheric studies, NASA/TM-104606. *Max J*, 19.
- 415 Elser, M., Huang, R. J., Wolf, R., Slowik, J. G., Wang, Q., Canonaco, F., Li, G., Bozzetti, C.,
416 Daellenbach, K. R., Huang, Y., Zhang, R., Li, Z., Cao, J., Baltensperger, U., El-Haddad,
417 I., and Prévôt, A. S. H., 2016. New insights into PM_{2.5} chemical composition and sources
418 in two major cities in China during extreme haze events using aerosol mass spectrometry.
419 *Atmospheric Chemistry and Physics*, 16, 3207-3225, doi: 10.5194/acp-16-3207-2016.
- 420 Fast, J. D., Jr, W. I. G., Easter, R. C., Zaveri, R. A., Barnard, J. C., Chapman, E. G., Grell, G.
421 A., and Peckham, S. E., 2006. Evolution of ozone, particulates, and aerosol direct
422 radiative forcing in the vicinity of Houston using a fully coupled meteorology-chemistry-
423 aerosol model. *Journal of Geophysical Research-Atmospheres*, 111(D21), doi:
424 10.1029/2005JD006721.
- 425 Feng, T., Li, G., Cao, J., Bei, N., Shen, Z., Zhou, W., Liu, S., Zhang, T., Wang, Y., Huang, R.
426 J., Tie, X., and Molina, L. T., 2016. Simulations of organic aerosol concentrations during
427 springtime in the Guanzhong Basin, China. *Atmospheric Chemistry and Physics*, 16,
428 10045-10061, doi: 10.5194/acp-16-10045-2016.
- 429 Gao, M., Carmichael, G. R., Wang, Y., Saide, P. E., Yu, M., Xin, J., Liu, Z., and Wang, Z.,
430 2016. Modeling study of the 2010 regional haze event in the North China Plain,
431 *Atmospheric Chemistry and Physics*, 16(3), 1673-1691, doi: 10.5194/acp-16-1673-2016.
- 432 Ge, S., Xu, X., Chow, J.C., Watson, J., Sheng, Q., Liu, W., Bai, Z., Zhu, T., and Zhang, J.,
433 2004. Emissions of air pollutants from household Stoves: honeycomb coal versus coal
434 cake. *Environmental Science and Technology*, 38(17), 4612-4618, doi:
435 10.1021/es049942k.
- 436 Grell, G. A., Peckham, S. E., Schmitz, R., McKeen, S. A., Frost, G., Skamarock, W. C., and
437 Eder, B., 2005. Fully coupled "online" chemistry within the WRF model. *Atmospheric*
438 *Environment*, 39, 6957-6975, doi: 10.1016/j.atmosenv.2005.04.027.
- 439 Guenther, A., Karl, T., Harley, P., Wiedinmyer, C., Palmer, P. I., and Geron, C., 2006.
440 Estimates of global terrestrial isoprene emissions using MEGAN (Model of Emissions of
441 Gases and Aerosols from Nature). *Atmospheric Chemistry and Physics*, 6, 3181-3210,
442 doi: 10.5194/acp-6-3181-2006.
- 443 Guo, S., Hu, M., Wang, Z. B., Slanina, J., and Zhao, Y. L., 2010. Size-resolved aerosol water-
444 soluble ionic compositions in the summer of Beijing: implication of regional secondary
445 formation. *Atmospheric Chemistry and Physics*, 10, 947-959, doi:10.5194/acp-10-947-
446 2010.



- 447 Guo, S., Hu, M., Zamora, M. L., Peng, J., Shang, D., Zheng, J., Du, Z. F., Wu, Z., Shao, M.,
448 Zeng, L. M., Molina, M. J., and Zhang, R. Y., 2014. Elucidating severe urban haze
449 formation in China. *Proceedings of the National Academy of Sciences of the United*
450 *States of America*, 111(49), 17373-17378, doi: 10.1073/pnas.1419604111.
- 451 Hong, S. Y. and Lim, J. O. J., 2006. The WRF Single-Moment 6-Class Microphysics Scheme
452 (WSM6). *Asia-Pacific Journal of Atmospheric Sciences*, 42, 129-151.
- 453 Horowitz, L. W., Walters, S., Mauzerall, D. L., Emmons, L. K., Rasch, P. J., Granier, C., Tie,
454 X. X., Lamarque, J. F., Schultz, M. G., Tyndall, G. S., Orlando, J. J., and Brasseur, G. P.,
455 2003. A global simulation of tropospheric ozone and related tracers: Description and
456 evaluation of MOZART, version 2. *Journal of Geophysical Research*, 108, 4784, doi:
457 10.1029/2002jd002853.
- 458 Huang, R. J., Zhang, Y., Bozzetti, C., Ho, K. F., Cao, J. J., Han, Y. M. Daellenbach, K. R.,
459 Slowik, J. G., Platt, S. M., Canonaco, F., Zotter, P., Wolf, R., Pieber, S. M., Bruns, E. A.,
460 Crippa, M., Ciarelli, G., Piazzalunga, A., Schwikowski, M., Abbaszade, G., Schnelle-
461 Kreis, J., Zimmermann, R., An, Z. S., Szidat, S., Baltensperger, U., El Haddad, I., and
462 Prevot, A. S. H., 2014. High secondary aerosol contribution to particulate pollution
463 during haze events in China. *Nature*, 514(7521), 218-222, doi: 10.1038/nature13774.
- 464 Janjić, Z. I., 2002. Nonsingular Implementation of the Mellor-Yamada Level 2.5 Scheme in
465 the NCEP Meso Model. *Ncep Office Note*, 436 pp.
- 466 Lei, Y., Zhang, Q., He, K. B., and Streets, D. G., 2011. Primary anthropogenic aerosol
467 emission trends for China, 1990-2005. *Atmospheric Chemistry and Physics*, 11(3), 931-
468 954, doi: 10.5194/acp-11-931-2011.
- 469 Li, G., Bei, N., Tie, X., and Molina, L. T., 2011a. Aerosol effects on the photochemistry in
470 Mexico City during MCMA-2006/MILAGRO campaign. *Atmospheric Chemistry and*
471 *Physics*, 11, 5169-5182, doi: 10.5194/acp-11-5169-2011.
- 472 Li, G., Lei, W., Zavala, M., Volkamer, R., Dusanter, S., Stevens, P., and Molina, L. T., 2010.
473 Impacts of HONO sources on the photochemistry in Mexico City during the MCMA-
474 2006/MILAGO Campaign. *Atmospheric Chemistry and Physics*, 10, 6551-6567, doi:
475 10.5194/acp-10-6551-2010.
- 476 Li, G., Zavala, M., Lei, W., Tsimpidi, A. P., Karydis, V. A., Pandis, S. N., Canagaratna, M. R.,
477 and Molina, L. T., 2011b. Simulations of organic aerosol concentrations in Mexico City
478 using the WRF- CHEM model during the MCMA-2006/MILAGRO campaign.
479 *Atmospheric Chemistry and Physics*, 11, 3789-3809, doi: 10.5194/acp-11-3789-2011.
- 480 Li, G., Zhang, R., Fan, J., and Tie, X., 2005. Impacts of black carbon aerosol on photolysis
481 and ozone. *Journal of Geophysical Research Atmospheres*, 110, D23206, doi:
482 10.1029/2005JD005898.
- 483 Li, J., Huang, X., Yang, H., Chuai, X., Li, Y., Qu, J., and Zhang, Z., 2016. Situation and
484 determinants of household carbon emissions in Northwest China. *Habitat International*,
485 51, 178-187, doi: 10.1016/j.habitatint.2015.10.024.
- 486 Li, M., Zhang, Q., Kurokawa, J. I., Woo, J. H., He, K., Lu, Z., Ohara, T., Song, Y., Streets, D.
487 G., Carmichael, G. R., Cheng, Y., Hong, C., Huo, H., Jiang, X., Kang, S., Liu, F., Su, H.,
488 and Zheng, B., 2017. MIX: a mosaic Asian anthropogenic emission inventory under the



- 489 international collaboration framework of the MICS-Asia and HTAP. *Atmospheric*
490 *Chemistry and Physics*, 17, 935-963, doi: 10.5194/acp-17-935-2017.
- 491 Li, X., Zhang, Q., Zhang, Y., Zheng, B., Wang, K., and Chen, Y. 2015. Source contributions
492 of urban PM_{2.5} in the Beijing-Tianjin-Hebei region: Changes between 2006 and 2013 and
493 relative impacts of emissions and meteorology. *Atmospheric Environment*, 123, 229-239,
494 doi: 10.1016/j.atmosenv.2015.10.048.
- 495 Liu, F., Zhang, Q., Tong, D., Zheng, B., Li, M., Huo, H., and He, K. B., 2015. High-
496 resolution inventory of technologies, activities, and emissions of coal-fired power plants
497 in China from 1990 to 2010. *Atmospheric Chemistry and Physics*, 15(23), 13299-13317,
498 doi:10.5194/acp-15-13299-2015.
- 499 Liu, J., Mauzerall, D. L., Chen, Q., Zhang, Q., Song, Y., Peng, W., Klimont, Z., Qiu, X. H.,
500 Zhang, S. Q., Hu, M., Lin, W. L., Smith, K. R., Zhu, T., 2016. Air pollutant emissions
501 from Chinese households: a major and underappreciated ambient pollution source.
502 *Proceedings of the National Academy of Sciences of the United States of America*,
503 113(28), 7756-7761, doi: 10.1073/pnas.1604537113.
- 504 Long, X., Tie, X., Cao, J., Huang, R., Feng, T., Li, N., Zhao, S., Tian, J., Li, G., and Zhang,
505 Q., 2016. Impact of crop field burning and mountains on heavy haze in the North China
506 Plain: a case study. *Atmospheric Chemistry and Physics*, 16, 9675-9691, doi:
507 10.5194/acp-16-9675-2016.
- 508 Lv, B., Zhang, B., and Bai, Y., 2016. A systematic analysis of PM_{2.5} in Beijing and its sources
509 from 2000 to 2012. *Atmospheric Environment*, 124, 98-108, doi:
510 10.1016/j.atmosenv.2015.09.031.
- 511 Ma, Q., Cai, S., Wang, S., Zhao, B., Martin, R. V., Brauer, M., Cohen, A., Jiang, J., Zhou, W.,
512 Hao, J., Frostad, J., Forouzanfar, M. H., and Burnett, R. T., 2017. Impacts of coal burning
513 on ambient PM_{2.5} pollution in China. *Atmospheric Chemistry and Physics*, 17, 4477-
514 4491, doi: 10.5194/acp-17-4477-2017.
- 515 Ministry of Environmental Protection of China (MEP): 2013 Report on the State of
516 Environment in China, 2014 (in Chinese).
- 517 Ministry of Environmental Protection of China (MEP): 2014 Report on the State of
518 Environment in China, 2015 (in Chinese).
- 519 Nenes, A., Pandis, S. N., and Pilinis, C., 1998. ISORROPIA: A new thermodynamic
520 equilibrium model for multiphase multi-component inorganic aerosols. *Aquatic*
521 *Geochemistry*, 4, 123-152, doi: 10.1023/a:1009604003981.
- 522 Quan, J., Tie, X., Zhang, Q., Liu, Q., Li, X., Gao, Y., and Zhao, D. L., 2014. Characteristics
523 of heavy aerosol pollution during the 2012-2013 winter in Beijing, China. *Atmospheric*
524 *Environment*, 88(5), 83-89, doi: 10.1016/j.atmosenv.2014.01.058.
- 525 Seinfeld, J. H. and Pandis, S. N., 2006. Atmospheric Chemistry and Physics: From Air
526 Pollution to Climate Change, 2nd Edition. *Wiley*.
- 527 Sheehan, P., Cheng, E., English, A., and Sun, F., 2014. China's response to the air pollution
528 shock. *Nature Climate Change*, 4(5):306-309, doi: 10.1038/nclimate2197.



- 529 Shen, G., Yang, Y., Wang, W., Tao, S., Zhu, C., Min, Y., Xue, M., Ding, J., Wang, B., Wang,
530 R., Shen, H., Li, W., Wang, X., and Russell, A.G., 2010. Emission factors of particulate
531 matter and elemental carbon for crop residues and coals burned in typical household
532 stoves in China. *Environmental Science and Technology*, 44(18), 7157-7162, doi:
533 10.1021/es101313y.
- 534 Tie, X., Madronich, S., Walters, S., Zhang, R. Y., Rasch, P., and Collins, W., 2003. Effect of
535 clouds on photolysis and oxidants in the troposphere. *Journal of Geophysical Research*,
536 108, 4642, doi: 10.1029/2003jd003659.
- 537 Wang, G. H., Zhang, R. Y., Gomez, M. E., Yang, L. X., Zamora, M. L., Hu, M., Lin, Y., Peng,
538 J. F., Guo, S., Meng, J. J., Li, J. J., Cheng, C. L., Hu, T. F., Ren, Y. Q., Wang, Y. S., Gao,
539 J., Cao, J. J., An, Z. S., Zhou, W. J., Li, G. H., Wang, J. Y., Tian, P. F., Marrero-Ortiz, W.,
540 Secrest, J., Du, Z. F., Zheng, J., Shang, D. J., Zeng, L. M., Shao, M., Wang, W. G.,
541 Huang, Y., Wang, Y., Zhu, Y. J., Li, Y. X., Hu, J. X., Pan, B., Cai, L., Cheng, Y. T., Ji, Y.
542 M., Zhang, F., Rosenfeld, D., Liss, P. S., Duce, R. A., Kolb, C. E., and Molina, M. J.,
543 2016. Persistent sulfate formation from London fog to Chinese haze. *Proceedings of the*
544 *National Academy of Sciences of the United States of America*, 113(48), 13630-13635,
545 doi: 10.1073/pnas.1616540113.
- 546 Wang, L. T., Wei, Z., Yang, J., Zhang, Y., Zhang, F. F., Su, J., Meng, C. C., and Zhang, Q.,
547 2014. The 2013 severe haze over southern Hebei, China: model evaluation, source
548 apportionment, and policy implications, *Atmospheric Chemistry and Physics*, 14, 3151-
549 3173, doi: 10.5194/acp-14-3151-2014.
- 550 Wang, L. T., Xu, J., Yang, J., Zhao, X. J., Wei, W., Cheng, D. D., Pan, X. M., and Su, J.,
551 2012. Understanding haze pollution over the southern Hebei area of China using the
552 CMAQ model. *Atmospheric Environment*, 56(5), 69-79, doi:
553 10.1016/j.atmosenv.2012.04.013.
- 554 Wang, X., Carmichael, G., Chen, D., Tang, Y., and Wang, T., 2005. Impacts of different
555 emission sources on air quality during March 2001 in the Pearl River Delta (PRD)
556 region. *Atmospheric Environment*, 39, 5227-5241, doi: 10.1016/j.atmosenv.2005.04.035.
- 557 Wesely, M. L., 1989. Parameterization of surface resistances to gaseous dry deposition in
558 regional-scale numerical models. *Atmospheric Environment*, 23, 1293-1304, doi:
559 10.1016/0004-6981(89)90153-4.
- 560 WHO, (World Trade Organization), 2005. Air Quality Guidelines for Particulate Matter,
561 Ozone, Nitrogen Dioxide and Sulfur Dioxide.
- 562 Williams, L. R., Gonzalez, L. A., Peck, J., Trimborn, D., McInnis, J., Farrar, M. R., Moore, K.
563 D., Jayne, J. T., Robinson, W. A., Lewis, D. K., Onasch, T. B., Canagaratna, M. R.,
564 Trimborn, A., Timko, M. T., Magoon, G., Deng, R., Tang, D., Blanco, E., Prevot, A. S. H.,
565 Smith, K. A., and Worsnop, D. R.: Characterization of an aerodynamic lens for
566 transmitting particles greater than 1 micrometer in diameter into the Aerodyne aerosol mass
567 spectrometer, *Atmos. Meas. Tech.*, 6(11), 3271-3280, 2013.
- 568 Wornat, M. J., Ledesma, E. B., Sandrowitz, A. K., Roth, M. J., Dawsey, S. M., Qiao, Y. L.,
569 and Chen, W., 2001. Polycyclic aromatic hydrocarbons identified in soot extracts from
570 domestic coal-burning stoves of Henan province, China. *Environmental Science and*
571 *Technology*, 35(10), 1943-1952, doi: 10.1021/es001664b.



- 572 Wu, J., Li, G., Cao, J., Bei, N., Wang, Y., Feng, T., Huang, R., Liu, S., Zhang, Q., and Tie, X.,
573 2017. Contributions of trans-boundary transport to summertime air quality in Beijing,
574 China. *Atmospheric Chemistry and Physics*, 17, 2035-2051, doi:10.5194/acp-17-2035-
575 2017.
- 576 Xue, Y. F., Zhou, Z., Nie, T., Wang, K., Nie, L., Pan, T., Wu, X. Q., Tian, H. Z., Zhong, L. H.,
577 Li, J., Liu, H. J., Liu, S. H., and Shao, P. Z., 2016. Trends of multiple air pollutants
578 emissions from residential coal combustion in Beijing and its implication on improving
579 air quality for control measures. *Atmospheric Environment*, 142, 303-312, doi:
580 10.1016/j.atmosenv.2016.08.004.
- 581 Yang, H., Chen, J., Wen, J., Tian, H., and Liu, X., 2016. Composition and sources of PM_{2.5},
582 around the heating periods of 2013 and 2014 in Beijing: implications for efficient
583 mitigation measures. *Atmospheric Environment*, 124, 378-386, doi:
584 10.1016/j.atmosenv.2015.05.015.
- 585 Zhang, L., Liu, L., Zhao, Y., Gong, S., Zhang, X., Henze, D. K., Capps, S. L., Fu, T. M.,
586 Zhang, Q. and Wang, Y., 2015. Source attribution of particulate matter pollution over
587 North China with the adjoint method. *Environmental Research Letters*, 10(8), 084011,
588 doi: 10.1088/1748-9326/10/8/084011.
- 589 Zhang, L., Wang, T., Lv, M., and Zhang, Q., 2015. On the severe haze in Beijing during
590 January 2013: unraveling the effects of meteorological anomalies with WRF-Chem.
591 *Atmospheric Environment*, 104, 11-21, doi: 10.1016/j.atmosenv.2015.01.001.
- 592 Zhang, Q., He, K., and Huo, H., 2012. Policy: cleaning china's air. *Nature*, 484(7393), 161-
593 162, doi: 10.1038/484161a.
- 594 Zhang, Q., Streets, D. G., Carmichael, G. R., He, K. B., Huo, H., Kannari, A., Klimont, Z.,
595 Park, I. S., Reddy, S., Fu, J. S., Chen, D., Duan, L., Lei, Y., Wang, L. T., and Yao, Z. L.,
596 2009. Asian emissions in 2006 for the NASA INTEX-B mission. *Atmospheric Chemistry
597 and Physics*, 9, 5131-5153, doi: 10.5194/acp-9-5131-2009.
- 598 Zhang, R., Jing, J., Tao, J., Hsu, S. C., Wang, G., Cao, J., Lee, C. S. L., Zhu, L., Chen, Z.,
599 Zhao, Y., and Shen, Z., 2013. Chemical characterization and source apportionment of
600 PM_{2.5} in Beijing: seasonal perspective. *Atmospheric Chemistry and Physics*, 13, 7053-
601 7074, doi:10.5194/acp-13-7053-2013.
- 602 Zhang, R., Wang, L., Khalizova, A. F., Zhao, J., Zheng, J., Mc-Grawb, R. L., and Molina, L.
603 T., 2009. Formation of nanoparticles of blue haze enhanced by anthropogenic pollution.
604 *Proceedings of the National Academy of Sciences of the United States of America*, 106,
605 17650-17654.
- 606 Zhang, X. Y., Wang, Y. Q., Niu, T., Zhang, X. C., Gong, S. L., Zhang, Y. M., and Sun, J. Y.,
607 2012. Atmospheric aerosol compositions in China: spatial/temporal variability, chemical
608 signature, regional haze distribution and comparisons with global aerosols. *Atmospheric
609 Chemistry and Physics*, 11(14), 26571-26615, doi: 10.5194/acpd-11-26571-2011.
- 610 Zhi, G., Chen, Y., Feng, Y., Xiong, S., Li, J., Zhang, G., Sheng, G., and Fu, J., 2008. Emission
611 characteristics of carbonaceous particles from various residential coal-stoves in China.
612 *Environmental Science and Technology*, 42(9), 3310-3315, doi: 10.1021/es702247q.
- 613 Zíková, N., Wang, Y., Yang, F., Li, X., Tian, M., and Hopke, P. K., 2016. On the source



614 contribution to Beijing PM_{2.5} concentrations. *Atmospheric Environment*, 134, 84-95, doi:
615 10.1016/j.atmosenv.2016.03.047.

616

617

618

619

620



621 Table 1 WRF-CHEM model configurations.

622

Region	Beijing-Tianjin-Hebei (BTH)
Simulation period	January 9 to 26, 2014
Domain size	150 × 150
Domain center	39°N, 117°E
Horizontal resolution	6km × 6km
Vertical resolution	35 vertical levels with a stretched vertical grid with spacing ranging from 30 m near the surface, to 500 m at 2.5 km and 1 km above 14 km
Microphysics scheme	WSM 6-class graupel scheme (Hong and Lim, 2006)
Boundary layer scheme	MYJ TKE scheme (Janjić, 2002)
Surface layer scheme	MYJ surface scheme (Janjić, 2002)
Land-surface scheme	Unified Noah land-surface model (Chen and Dudhia, 2001)
Longwave radiation scheme	Goddard longwave scheme (Chou and Suarez, 2001)
Shortwave radiation scheme	Goddard shortwave scheme (Chou and Suarez, 1999)
Meteorological boundary and initial conditions	NCEP 1°×1° reanalysis data
Chemical initial and boundary conditions	MOZART 6-hour output (Horowitz et al., 2003)
Anthropogenic emission inventory	Developed by Zhang et al. (2009) and Li et al. (2017)
Biogenic emission inventory	MEGAN model developed by Guenther et al. (2006)

623

624

625

626

627



628 Table 2 Average mass concentrations of air pollutants in REF case and SEN-BTH case from 9
629 to 25 January 2014 in BTH and Beijing. (Unit: $\mu\text{g m}^{-3}$ for $\text{PM}_{2.5}$, O_3 , NO_2 , SO_2 and mg m^{-3}
630 for CO)
631
632

Air pollutants	BTH				Beijing			
	REF	SEN-BTH	Mass change	Percentage change	REF	SEN-BTH	Mass change	Percentage change
$\text{PM}_{2.5}$	111.6	85.8	25.8	23.1%	97.7	68.9	28.8	29.5%
O_3	39.1	39.4	-0.3	-0.8%	39.3	39.8	-0.5	-1.3%
NO_2	45.7	43.7	2.0	4.3%	51.5	49.4	2.1	4.1%
SO_2	45.0	28.9	16.1	35.8%	42.2	24.2	18.0	42.6%
CO	1.7	1.3	0.4	22.5%	1.5	1.1	0.4	26.5%

633
634
635
636
637

**Figure Captions**

638

639

640 Figure 1 (a) Map showing the location of Beijing-Tianjin-Hebei and (b) WRF-CHEM model
641 simulation domain with topography. In (b), the filled red circles represent centers of
642 cities with ambient monitoring site and the size of the circle denotes the number of
643 ambient monitoring sites of cities. The filled black rectangle denotes the deployment
644 location of the HR-ToF-AMS in Beijing.

645 Figure 2 Pattern comparisons of simulated (color counters) vs. observed (colored circles)
646 near-surface mass concentrations of (a) $PM_{2.5}$, (b) O_3 , (c) NO_2 , and (d) SO_2
647 averaged from 9 to 25 January 2014. The black arrows indicate simulated surface
648 winds.

649 Figure 3 Comparisons of observed (black dots) and simulated (solid red lines) diurnal profiles
650 of near-surface hourly mass concentrations of (a) $PM_{2.5}$, (b) O_3 , (c) NO_2 , (d) SO_2 ,
651 and (e) CO averaged at monitoring sites in BTH from 9 to 25 January 2014.

652 Figure 4 Comparisons of measured (black dots) and simulated (solid red lines) diurnal
653 profiles of (a) organic aerosol (OA), (b) coal combustion organic aerosol (CCOA),
654 (c) sulfate, (d) nitrate, and (e) ammonium in Beijing from 9 to 25 January 2014.

655 Figure 5 Chemical composition of $PM_{2.5}$ averaged from 9 to 25 January 2014 in (a) BTH and
656 (b) Beijing.

657 Figure 6 Spatial distribution of the average contribution of the RCC emission in BTH and its
658 surrounding areas to $PM_{2.5}$ concentrations from 9 to 25 January 2014.

659 Figure 7 Chemical composition of $PM_{2.5}$ from the RCC emission averaged from 9 to 25
660 January 2014 in (a) BTH and (b) Beijing.

661 Figure 8 Average contributions of the RCC emission in Beijing to the Beijing's $PM_{2.5}$
662 concentration under different haze pollution levels from 9 to 25 January 2014.

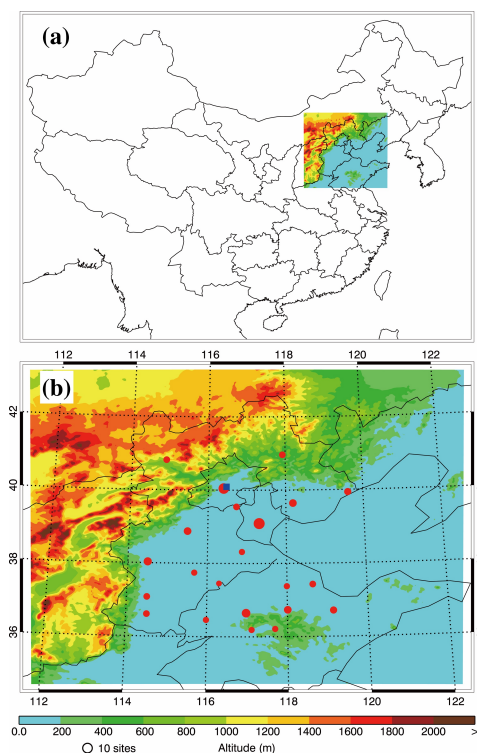
663

664

665

666

667



668

669

670

671 Figure 1 (a) Map showing the location of Beijing-Tianjin-Hebei and (b) WRF-CHEM model

672

673 simulation domain with topography. In (b), the filled red circles represent centers of cities

674

675 with ambient monitoring site and the size of the circle denotes the number of ambient

676

677

678

679

680

681

682

683

684

685

686

687

688

689

690

691

692

693

694

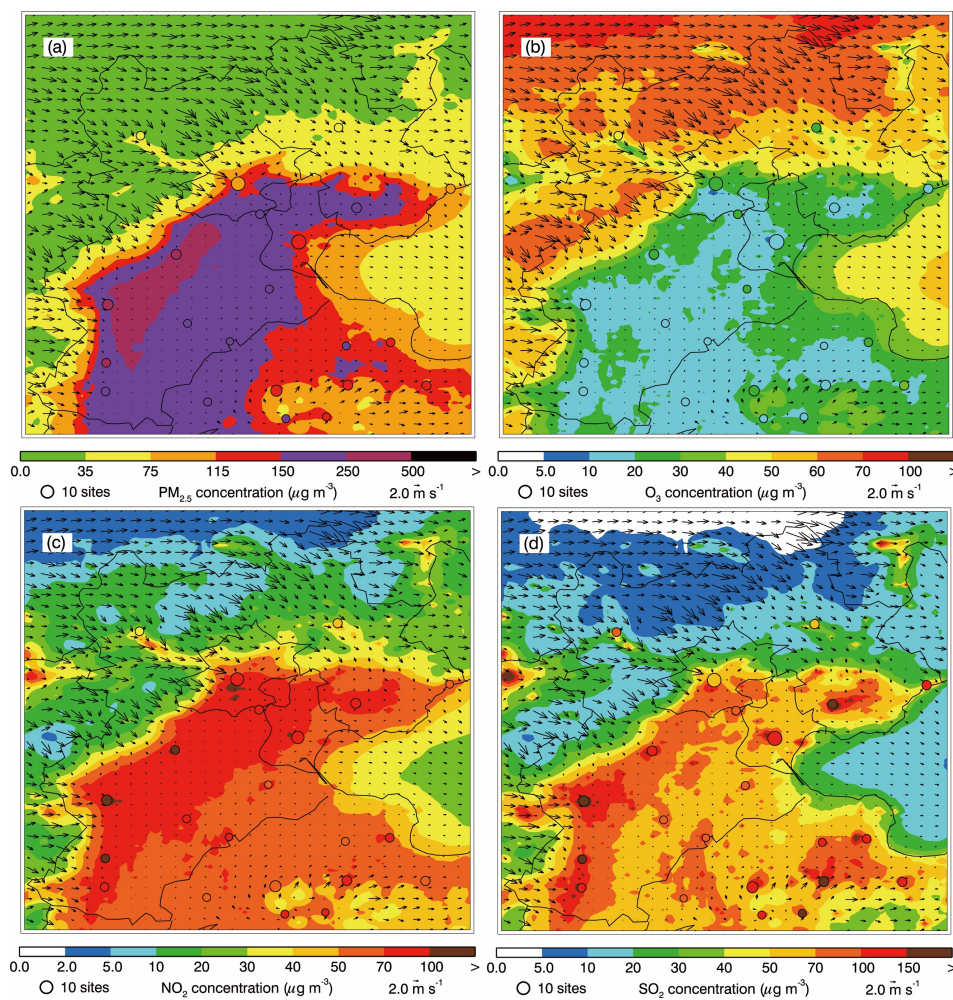
695

696

697

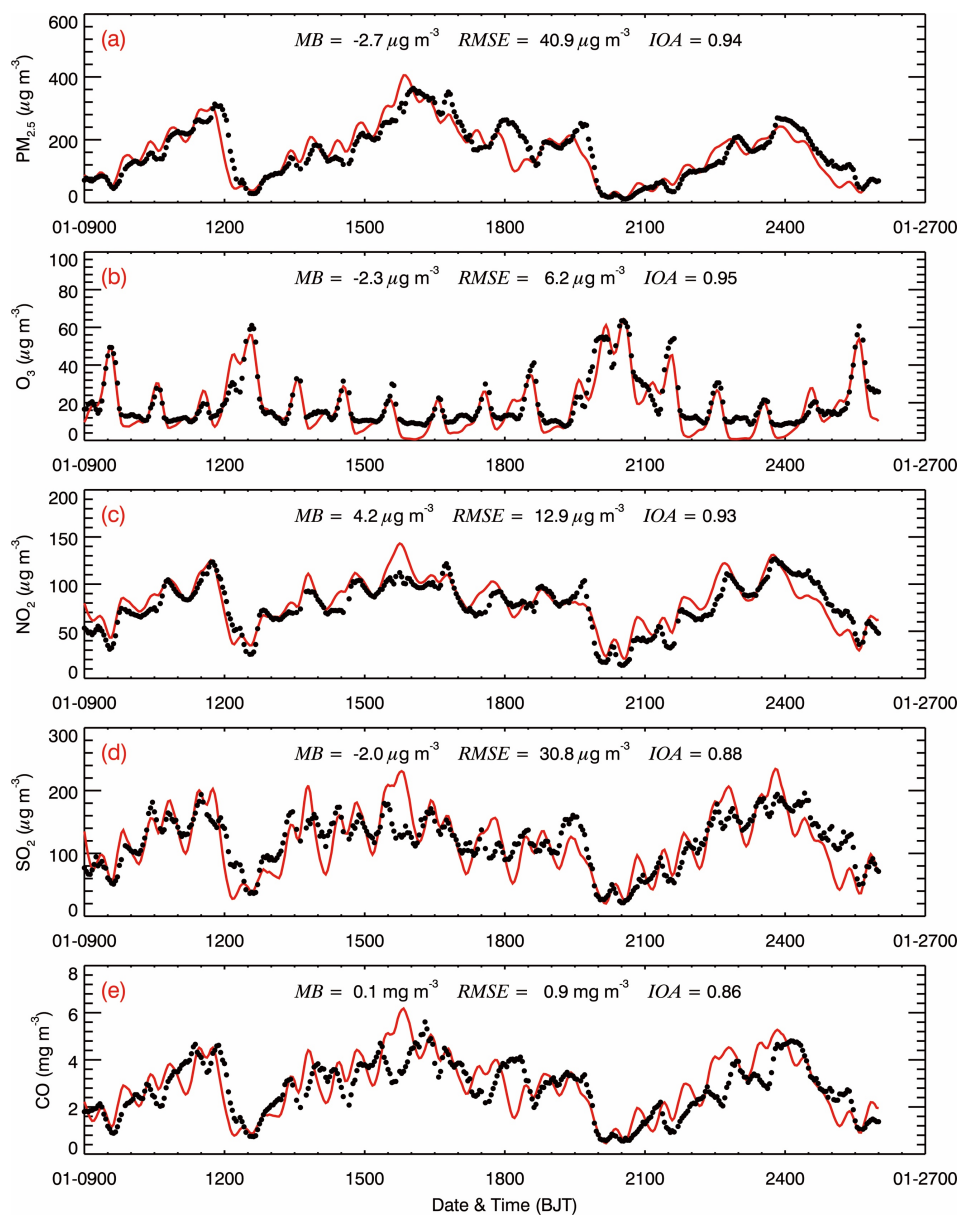
698

699



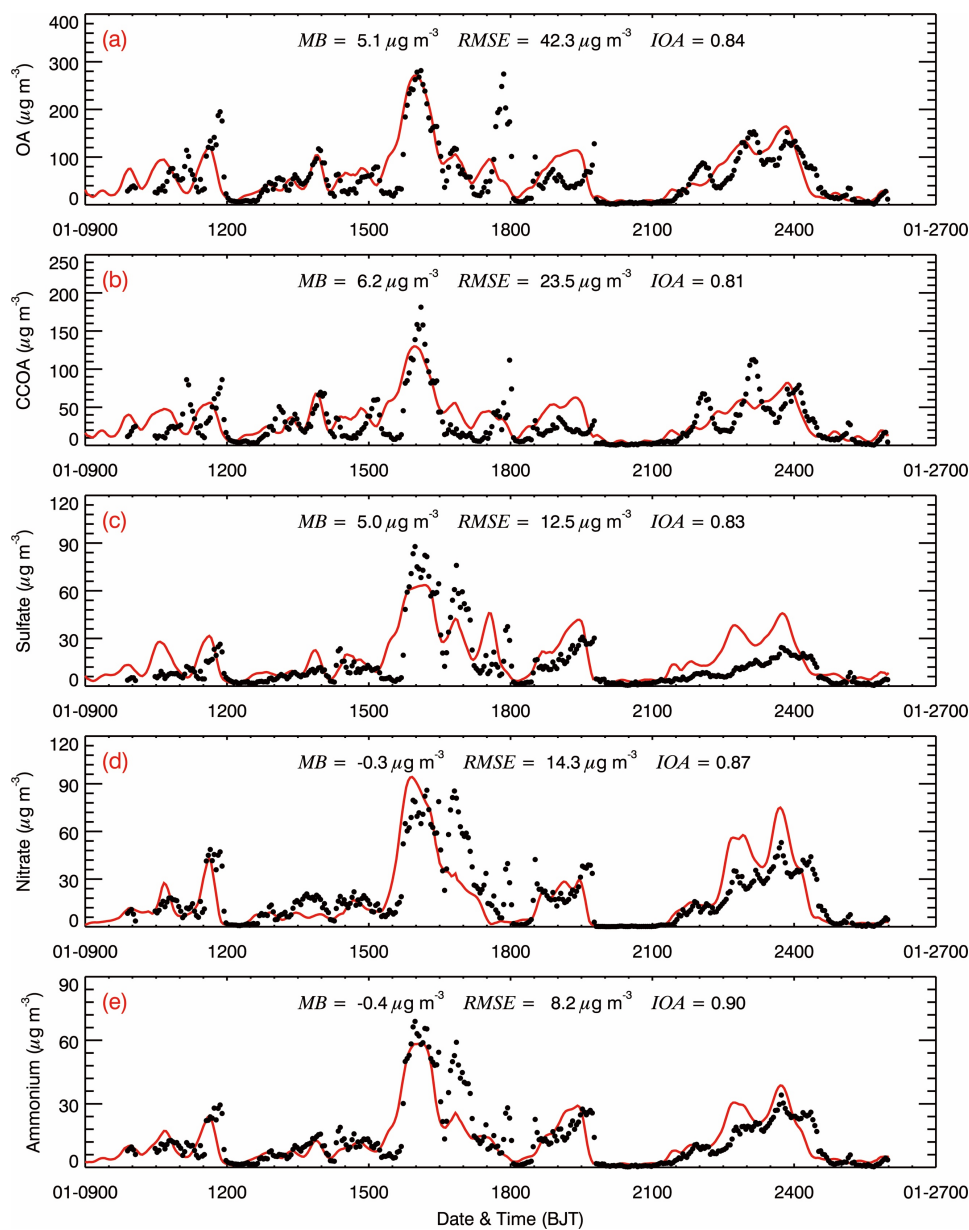
680
681
682
683
684
685
686
687
688
689

Figure 2 Pattern comparisons of simulated (color counters) vs. observed (colored circles) near-surface mass concentrations of (a) PM_{2.5}, (b) O₃, (c) NO₂, and (d) SO₂ averaged from 9 to 25 January 2014. The black arrows indicate simulated surface winds.



690
691
692
693
694
695
696
697
698
699

Figure 3 Comparisons of observed (black dots) and simulated (solid red lines) diurnal profiles of near-surface hourly mass concentrations of (a) $\text{PM}_{2.5}$, (b) O_3 , (c) NO_2 , (d) SO_2 , and (e) CO averaged at monitoring sites in BTH from 9 to 25 January 2014.



700

701 Figure 4 Comparisons of measured (black dots) and simulated (solid red lines) diurnal
702 profiles of (a) organic aerosol (OA), (b) coal combustion organic aerosol (CCOA), (c) sulfate,
703 (d) nitrate, and (e) ammonium in Beijing from 9 to 25 January 2014.

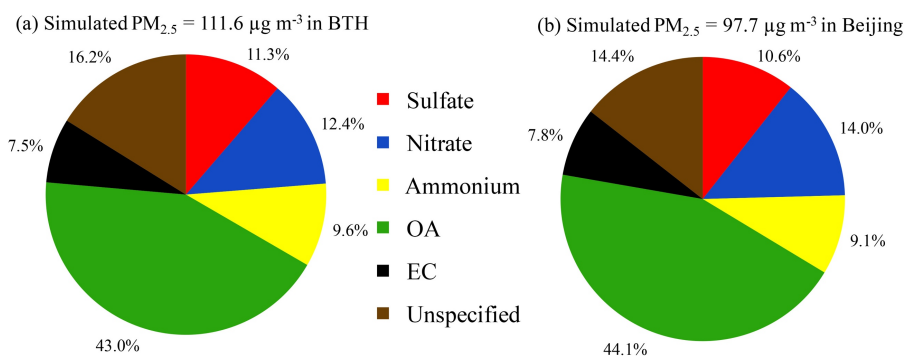
704

705

706

707

708



709

710

711 Figure 5 Chemical composition of $PM_{2.5}$ averaged from 9 to 25 January 2014 in (a) BTH and

712 (b) Beijing.

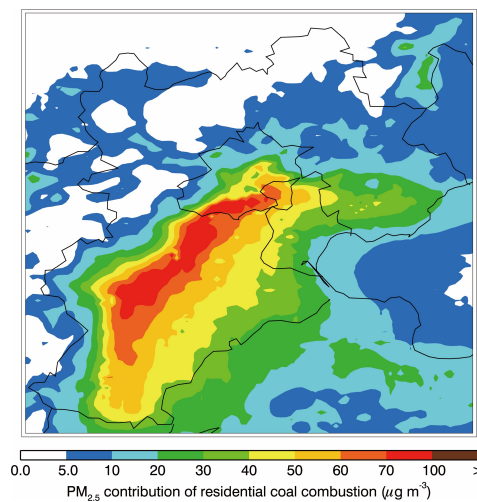
713

714

715

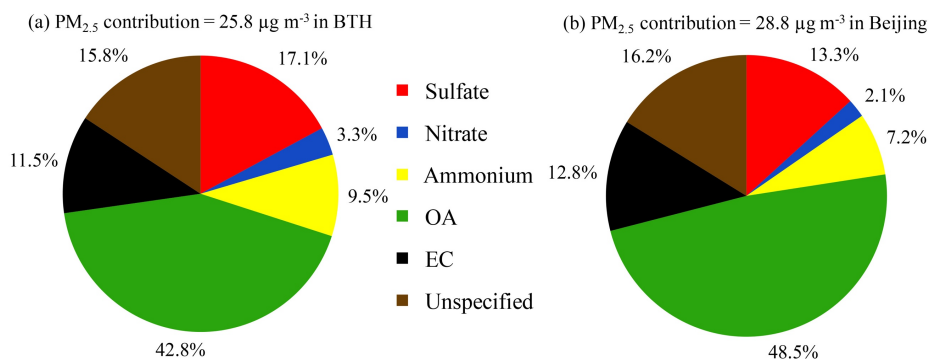
716

717



718
719
720
721
722
723
724
725
726

Figure 6 Spatial distribution of the average contribution of the RCC emission in BTH and its surrounding areas to $PM_{2.5}$ concentrations from 9 to 25 January 2014.



727

728 Figure 7 Chemical composition of PM_{2.5} from the RCC emission averaged from 9 to 25 January
729 2014 in (a) BTH and (b) Beijing.

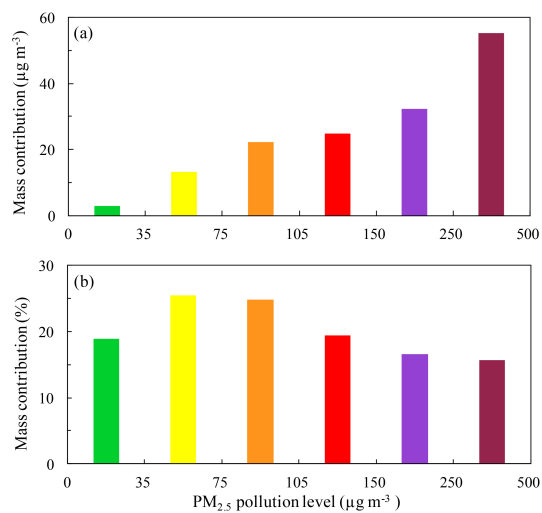
730

731

732

733

734



735

736

737 Figure 8 Average contributions of the RCC emission in Beijing to the Beijing's PM_{2.5}

738 concentration under different haze pollution levels from 9 to 25 January 2014.

739

740

741

742